CZECH TECHNICAL UNIVERSITY
IN PRAGUE

Faculty of Nuclear Sciences and Physical Engineering

Department of Physics

Research Project

Production of J/ψ in U+U collisions at the STAR Experiment

Author: Ota Kukral

Supervisor: RNDr. Petr Chaloupka, Ph.D.

Prague, 2013

ČESKÉ VYSOKÉ UČENÍ TECHNICKÉ
V PRAZE

Fakulta Jaderná a Fyzikálně Inženýrská

Katedra Fyziky

Výzkumný úkol

Produkce J/ψ ve srážkách U+U na experimentu STAR

Autor: Ota Kukral

Vedoucí práce: RNDr. Petr Chaloupka, Ph.D.

Praha, 2013

Acknowledgements

I would like to thank RNDr. Petr Chaloupka, Ph.D. for his persistent cooperation and additional guidance whenever a problem arose. He truly helped me to overcome the challenges of my first analysis.

I would also like to thank Mgr. Jaroslav Bielčík, Ph.D. for his suggestions and comments as well as for his continuous support.

Contents

Chapter 1

Motivation

One way to experimentally study properties of QCD matter is to collide heavy ions. In such collisions at sufficiently high energy, a novel state of matter, quark–gluon plasma (QGP) is created. It has been predicted that charmonium ($c\bar{c}$ bound state) would be suppressed due to in-medium dissociation caused by screening of color charge [1]. This screening is similar to a Debye screening of electric charge in plasma. It is described by Debye screening length λ_D. Charmonia start to dissolve if their radius is larger than λ_D. Different states of charmonium have different binding energies and radii. As a temperature of the system increases, λ_D decreases, therefore different states of charmonium are dissolved when different temperature of system has been reached starting from weakly bound. By observing which states have dissolved, the estimate of initial temperature of QGP can be obtained [2][3]. This mechanism applies not only to charmonia, but to other quarkonia as well.

To quantify this dissolution, p+p collisions, where it is expected that QGP is not created, are taken as a baseline. Production of a given particle in a collision of heavy ions is compared to its production in p+p collision. Nuclear modification factor R_{AA} is usually used:

$$R_{\mathrm{AA}}(p_{\mathrm{T}}, y) = \frac{\mathrm{d}^2 N^{\mathrm{AA}} / \mathrm{d}p_{\mathrm{T}}\,\mathrm{d}y}{N_{\mathrm{coll}}\,\mathrm{d}^2 N^{\mathrm{pp}} / \mathrm{d}p_{\mathrm{T}}\,\mathrm{d}y}. \tag{1.1}$$

It is the ratio of production in A+A collision to p+p collision scaled by number of binary collisions. If there wasn't any effect, this ratio should be exactly 1. In case that the particle is dissolved in A+A collision, R_{AA} would be less then 1 and we talk about suppression.

However, there are many competing mechanisms which can alter the particle production in A+A collisions such as initial-state nuclear effects on the

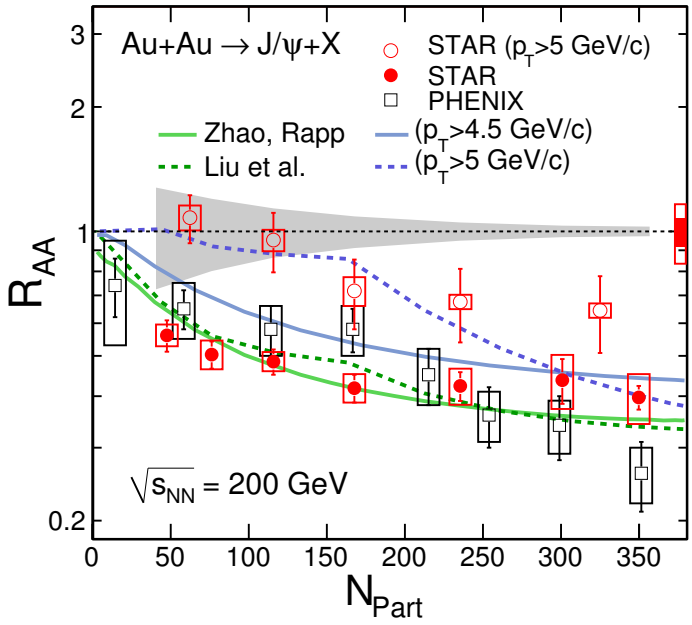

Figure 1.1: Nuclear modification factor R_{AA} for J/ψ in Au+Au at $\sqrt{s_{NN}}$ = 200 GeV. Results are shown for all p_{T} and for high p_{T} only. Lines depict comparison with two models [4][5]. Figure from [6].

parton distributions (shadowing), production via recombination of quark-antiquark pairs in the QGP or dissociation in hadronic phase. Therefore it is useful to study R_{AA} in various colliding systems. STAR has measured J/ψ in p+p, d+Au, Au+Au and Cu+Cu collisions at $\sqrt{s_{NN}}$ = 200 GeV [7][6] and Au+Au collisions at $\sqrt{s_{NN}}$ = 39 GeV and 62 GeV [8]. Fig. 1.1 shows dependence of J/ψ R_{AA} on number of participants and thus on centrality in Au+Au collisions at $\sqrt{s_{NN}}$ = 200 GeV. The results are for all p_{T} and for high p_{T} only. The suppression increases with centrality (R_{AA} decreases) and decreases for high p_{T}. Results are then compared to models that include contributions from prompt production and statistical charm quark regeneration [4][5].

Uranium collisions are of interest since uranium nucleus is non-spherical, which allows for more variability. One parameter (impact parameter) is not enough to describe the collision. Fig. 1.2 shows two prominent orientations which can happen during collision with centers of nuclei aligned. This non-spherical shape leads to higher initial energy density not only in tip-to-tip collision, but even when averaged over all possible orientations of incoming nuclei [9][10]. Fig. 1.3 compares multiplicities in Au+Au collision at $\sqrt{s_{NN}}$ = 200 GeV and U+U at $\sqrt{s_{NN}}$ = 193 GeV.

Figure 1.2: Two possible orientations (out of many) of colliding non-spherical nuclei of uranium.

Purpose of this analysis is to measure R_{AA} of J/ψ in U+U collisions at $\sqrt{s_{NN}} = 193$ GeV via dielectron decay channel J/$\psi \rightarrow \mathrm{e}^{+}\mathrm{e}^{-}$ and thus shed more light on the effects associated with in-medium dissociation of heavy quarkonia.

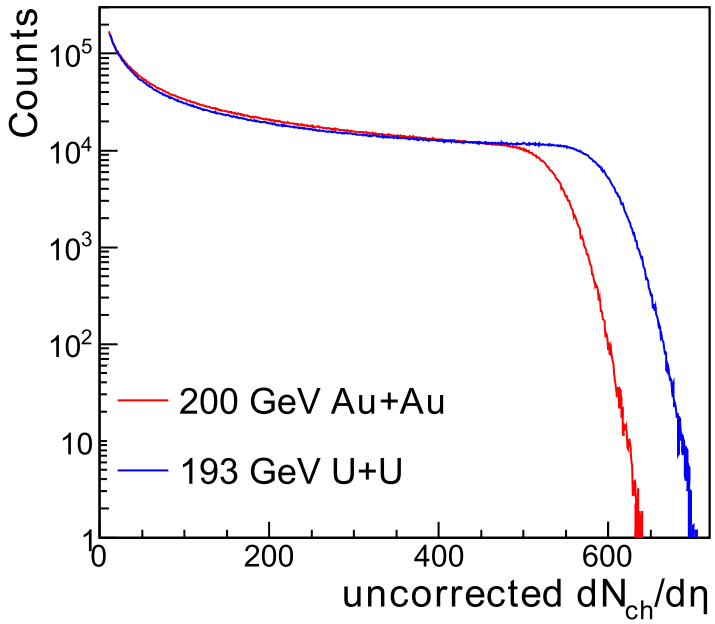

Figure 1.3: Uncorrected multiplicity for Au+Au collisions at $\sqrt{s_{NN}} = 200$ GeV and U+U collisions at $\sqrt{s_{NN}} = 193$ GeV. Figure from [10].

Chapter 2

STAR Experiment

STAR (Solenoid Tracker At RHIC) is a multi-purpose particle detector build to study high energy collisions. It is located in Relativistic Heavy Ion Collider (RHIC) in Brookhaven National Laboratory (BNL) on Long Island, NY, USA. It has been used for investigating diverse colliding systems, there have been collisions of p+p, d+Au, Au+Au, Cu+Cu and U+U at various energies. Fig. 2.1 shows position of STAR and other experiments at RHIC.

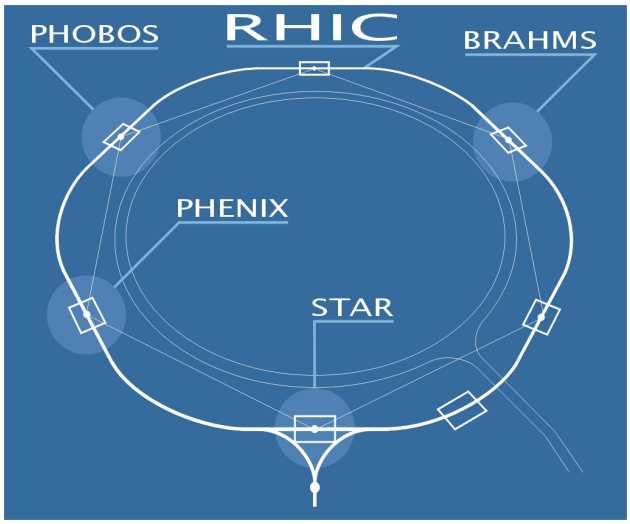

Figure 2.1: Relativistic Heavy Ion Collider with four original experiments. Currently only STAR and PHENIX are in operation.

STAR experiment consist of many different detectors and subsystems that serve different complementary purposes. The main are shown in Fig. 2.2.

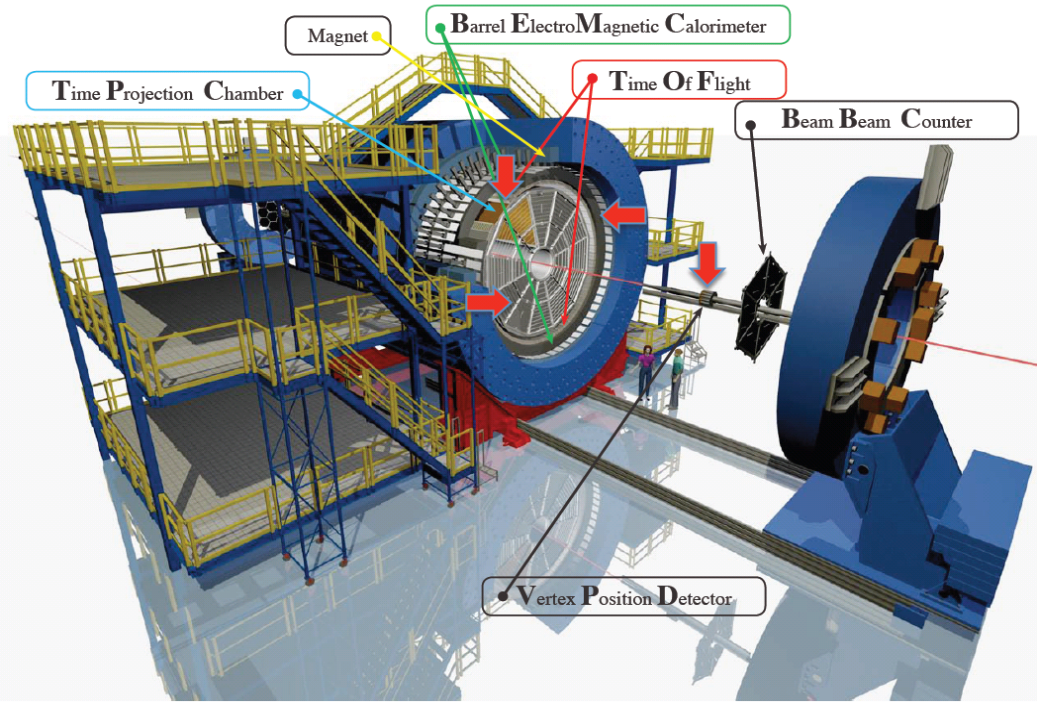

Figure 2.2: Depiction of STAR experiment showing names and positions of the main detectors.

2.1 Time Projection Chamber

Time Projection Chamber (TPC) is the main detector at the STAR experiment. It excels at charged particle tracking and momentum reconstruction, and also at particle identification via specific ionization loss $\mathrm{d}E/\mathrm{d}x$ at midrapidity. This allows for particle identification in a broad range of particle momenta as is ilustrated in Fig. 2.3. TPC is a cylinder with length of 420 cm covering 2π in azimuthal angle. Its inner radius is 50 cm, outer radius is 200 cm [11]. It is filled with a mixture of 10 % of methane and 90 % argon.

2.2 Time of Flight

Another main detector located at STAR is the Time of Flight (TOF) detector. Its main purpose is to improve particle identification by measuring their velocity β. It is based on Multi-gap Resistive Plate Chamber (MRPC) technology, which has been developed for LHC [12]. In principle, it is a stack of glass resistive plates with uniform gas gaps. Electric field is applied to the outer surface of the outer plates. When a charged particle goes through the

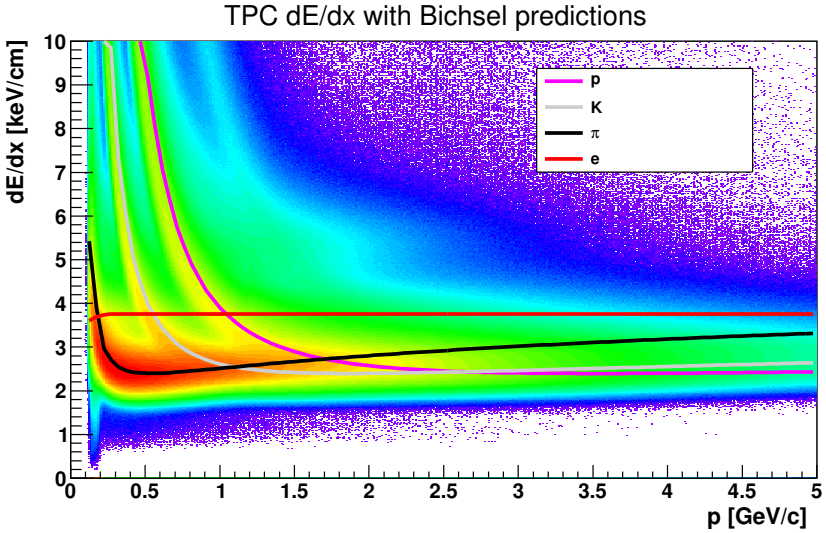

Figure 2.3: Dependence of ionization losses on momentum. Lines show theoretical predictions for various particle species. Picture was obtained from uranium collisions.

stack, it generates avalanches in the gas gaps. The glass plates are resistive and thus transparent to charge induction – induced signal is the sum of avalanches. The signal read out is provided by an array of copper pads. Since the detector has very fast timing resolution under 100 ps it is also used for event triggering.

2.3 Barrel Electromagnetic Calorimeter

Barrel Electromagnetic Calorimeter (BEMC) lies outside of TOF also covering 2π in azimuthal angle. It covers pseudorapidity $|\eta| < 1$. BEMC consists of 120 modules, each of which is formed by 40 towers[13]. Each tower spans $\approx 0,05$ in azimuthal angle and 0,05 in pseudorapidity. Towers are composed of 21 layers of lead alternating with 21 layers of scintillators. First 2 layers are read out separately as a preshower detector. There is also a Shower Maximum Detector between 5th and 6th layer, approximately in depth where the shower is the widest. BEMC is a fast detector, and is thus used for triggering.

2.4 Zero Degree Calorimeters

Zero Degree Calorimeters (ZDCs) are two hadron calorimeters positioned approximately 18 meters from interaction point on both sides of the detector. Their purpose is to detect spectator neutrons emitted within the cone along beam axis after the collision. They are placed directly in direction of the beam coming from the opposite side of the interaction point. The beam and charged spectators are deflected away by dipole magnet while neutrons continue their flight in straight line. Position so close to the beam trajectory limits ZDCs' width to 10 cm. The ZDC coincidence of the 2 beam directions is a minimum bias selection of heavy ion collision. This allows its use as a trigger [14].

2.5 Vertex Position Detector

Vertex Position Detector (VPD) consist of two plastic scintillators placed in the equal distance from the experiment center close to the beam axis. In high energy heavy ion collisions, large numbers of very forward and high energy photons are produced which travel from the collisions vertex as a prompt pulse. By measuring time at which these pulses reach two equally spaced detectors we can extract the primary vertex z position. Another use of VPD is to provide starting time for TOF measurement and due to its fast response it is used for triggering as well [15].

Chapter 3

J/ψ analysis

3.1 Data sample

This analysis was performed using minimum bias U+U collisions at $\sqrt{s_{NN}}$ = 193 GeV taken in 2012 by the STAR experiment at RHIC. The minimum bias events were selected using VPD and ZDC trigger. The total number of events with any accepted trigger was 377 millions. The distribution of uncorrected multiplicity is shown in Fig. 3.1

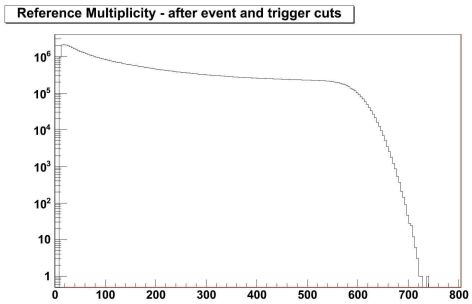

Figure 3.1: Distribution of uncorrected multiplicity for minimum bias triggers

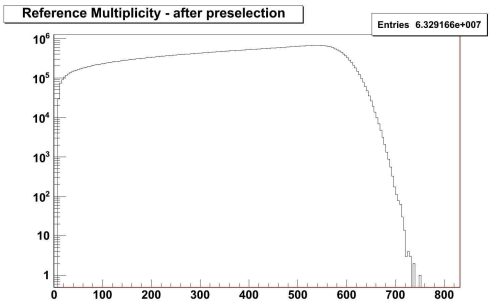

Figure 3.2: Distribution of uncorrected multiplicity after preselection, where only events with a suitable electron candidate are saved

3.1.1 Preselection

In STAR, data used for the analysis are stored in the data files called MuDST. However, these files are too large and contain much information unnecessary for this particular analysis. It is a common practice to extract

only information relevant for particular analysis from these files and store it in smaller files called PicoDST. Since the storage space is limited, we stored only events with at least one suitable electron candidate to further reduce amount of data to be saved. All cuts used in selecting suitable events were weaker than cuts used later in the actual analysis therefore the results are not affected by the preselection. The cuts are described in more detail in following sections. Fig. 3.2 shows the distribution of uncorrected multiplicity after the preselection, the increase in high multiplicity region is caused by higher probability of finding electron candidate in those events.

3.2 Event Cuts

Events are required to fulfill a few cuts to ensure their good quality. The events position has to be in the middle of the detector, its z distance (along the beam axis) from the center of the detector has to be smaller then 30 cm. Fig. 3.3 shows the distribution of the primary vertex position. Difference between reconstructed z position of the primary vertex by TPC and VPD has to be smaller then 3 cm in order to remove false pile-up events, the distribution is shown in Fig. 3.4.

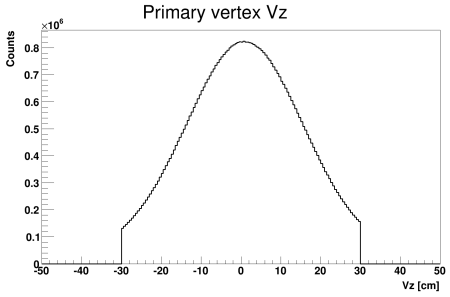

Figure 3.3: Distribution of primary vertex position

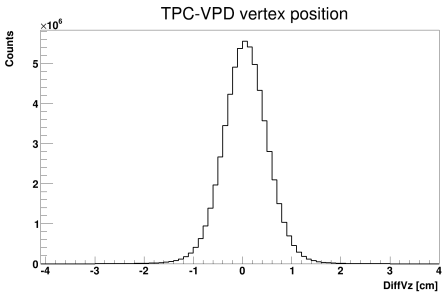

Figure 3.4: Difference between primary vertex z position as reconstructed by TPC and VPD.

Reference multiplicity of the event has to be larger than 10, this corresponds to 0-80 % of most central collisions. Centrality is discussed in more detail in following section.

3.3 Centrality selection

In the STAR experiment we select centrality of the event from its measured multiplicity. The relation between the observed number of particles and

the unobservable impact parameter is deduced from Monte Carlo Glauber model [16].Centrality regions are based on preliminary Matsui's work [17]. The multiplicity boundaries are summarized in Tab. 3.1:

% centrality	Multiplicity
5 %	> 535
10 %	> 466
15 %	> 399
20 %	> 339
25 %	> 283
30 %	> 233
35 %	> 189
40 %	> 151
45 %	> 118
50 %	> 91
55 %	> 68
60 %	> 50
65 %	> 35
70 %	> 24
75 %	> 16
80 %	> 10

Table 3.1: Multiplicity boundaries used in centrality definition.

Due to trigger inefficiencies for events with very low multiplicity, only events with multiplicity larger then 10 are considered thus limiting the analysis to 0-80 % of most central collisions.

3.4 Trajectory Cuts

There are several conditions that have to be fullfiled for a particle trajectory to be used. Number of fitted TPC hits has to be larger than 19 and ratio of fitted hits to maximum possible has to be larger than 0.51. This cut

ensures that we do not use tracks that would be obtained from a single track split artificially into two. Only primary trajectories are used. Each track is required to have the distance of closest approach (DCA) of trajectory to the primary vertex smaller than 3 cm. Pseudorapidity η of the trajectories has to be between -1 and 1. The mentioned distributions with apllied cut values are shown in Fig. 3.5 and 3.6.

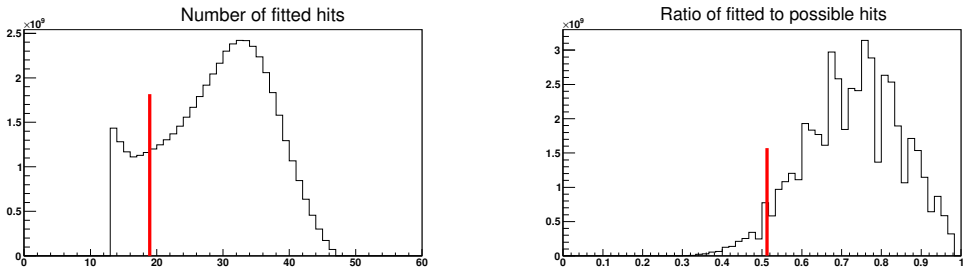

Figure 3.5: Left: Number of fitted hits in TPC. Right: Ratio of fitted to maximum possible hits in TPC. Red lines show cuts used.

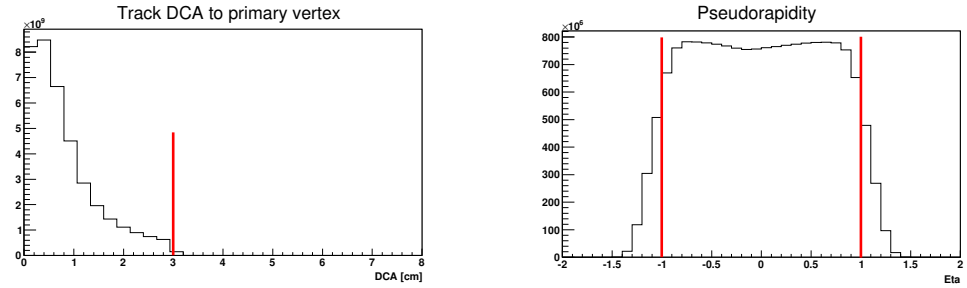

Figure 3.6: Left: Distance of closest approach of trajectory to primary vertex. Right: Pseudorapidity of primary tracks. Red lines show cuts used.

3.5 Electron Selection

From primary trajectories which passed the trajectory cut electrons are selected in order to reconstruct J/ψ via its dielectron decay channel. Data from TPC, TOF and BEMC are used for the electron identification. The detectors are described in chapter 2.

3.5.1 TPC

Particles can be identified by their specific ionization loss pattern in TPC. This ionization energy loss is expressed in $n\sigma$ units. For a given particle species and momentum, distribution of $\log(\mathrm{d}E/\,\mathrm{d}x)$ is supposed to have a Gaussian shape with a mean described by Bichsel function $B = f(p/m)$ and variance given by resolution of $\mathrm{d}E/\,\mathrm{d}x = \sigma$. Then $n\sigma$ is the distance from this mean expressed as a number of standard deviations:

$$n\sigma = \frac{\log((\mathrm{d}E/\,\mathrm{d}x)/B}{\sigma}. \tag{3.1}$$

In an ideal case $n\sigma$ has a normal distribution - mean is 0 and standard deviation is 1. In our analysis $n\sigma_e$ for electrons and $n\sigma_\pi$ for pions is used.

For electrons, $n\sigma_e$ is required to be $-1.5 < n\sigma_e < 2.0$. Fig. 3.7 shows the $n\sigma_e$ versus particle momentum after TOF and BEMC cuts have been applied. The figure also illustrates why asymmetric cut is used – the hadron contamination is larger from particles with lower dE/dx.

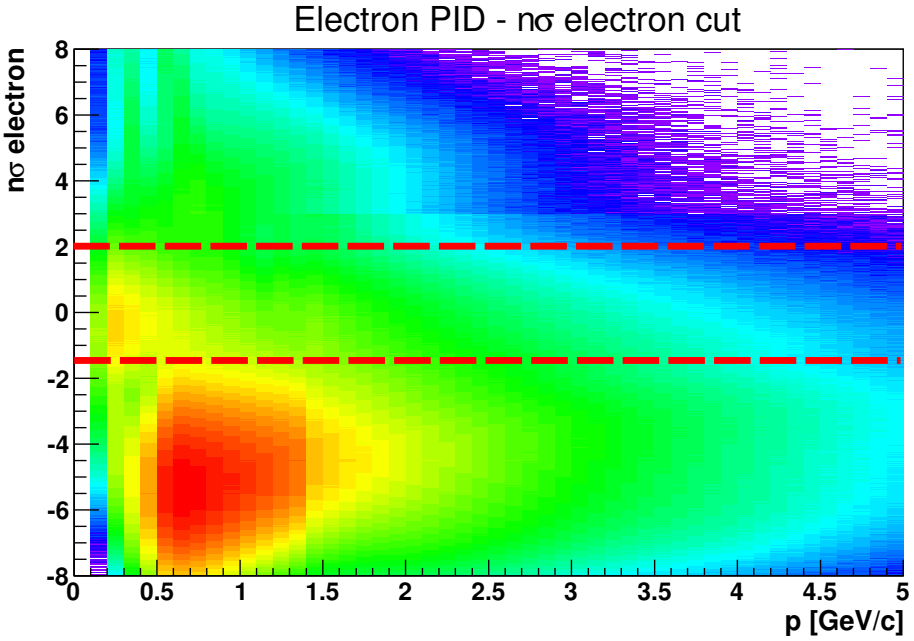

Figure 3.7: $n\sigma_e$ in logarithmic scale for particles which have already passed TOF and BEMC cuts. Red lines show $n\sigma_e$ cut.

The second used cut is $|n\sigma_\pi| > 2.5$. This cut helps to reduce the contamination of electrons by pions and plays a role for particles with $p \lesssim 0.2$ GeV/c or $p \gtrsim 3$ GeV/c where there are similar expected ionization losses for electrons and pions.

3.5.2 TOF

TOF detector is used to measure particle velocity β. Due to their low mass, electrons have $\beta \approx 1$ for the whole range of considered momenta. We require $0.97 < 1/\beta < 1.03$. For a particle to have a valid TOF signal, $|y_{\mathrm{local}}|$ <1.8 cm is demanded, where y_{local} is distance of the track projection and the center of TOF pad. This condition is there to remove false matches in the detector.

Particles with $p < 1.4$ GeV/c have to fulfill the TOF cut strictly. For particles with $p > 1.4$ GeV/c the advantage of using TOF is lower, since also pions have β close to 1 and dE/dx bands do not overlap in that momentum region. Therefore the cut is used for particles with $p > 1.4$ GeV/c only if they have a valid TOF signal. This prevents unnecessary diminishing of electron identification efficiency. Fig. 3.8 shows the TOF cut for particles that have already fulfilled TPC and BEMC cuts.

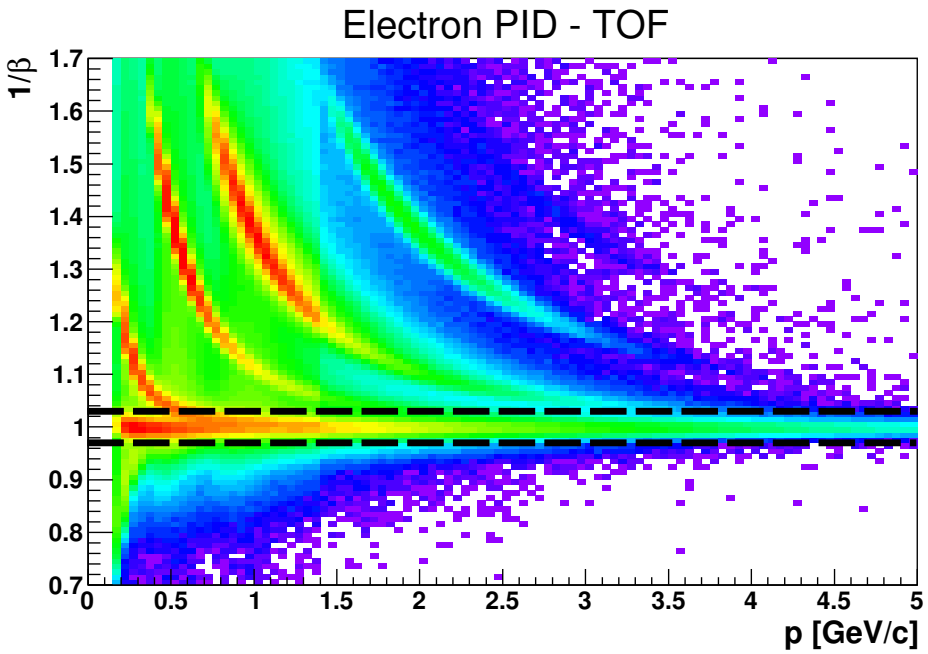

Figure 3.8: $1/\beta$ in logarithmic scale for particles which have already passed TPC and BEMC cuts. Black lines show TOF cut.

3.5.3 BEMC

BEMC is used to obtain an energy E which was deposited in a single tower. Electrons, unlike hadrons, are supposed to deposit all of their energy

in the calorimeter, hence having ratio $p/E \approx 1$. This can be used to further suppress hadron contamination in higher p. However, besides calorimeter resolution, there are two other effects which change the electron energy deposited in the calorimeter and thus p/E ratio. First, the electron energy can leak into neighboring towers, especially if the trajectory hits close to an edge of the tower. In this case, the registered E is smaller and p/E larger than 1. The other effect happens since U+U collisions are high multiplicity events: There can be energy registered in the tower, which comes from other particles hitting the calorimeter nearby. This makes p/E smaller than 1.

BEMC cut is used only for particles with $p > 1.4$ GeV/c. We require $0.3 < p/E < 1.5$ for the results presented in this research project, however the cut has changed several times and is currently $0.5 < p/E < 2$.

Chapter 4

Results

In this work we reconstruct J/ψ via dielectron decay channel $J/\psi \rightarrow e^+e^-$ with branching ratio 5.9 %. Electrons with opposite signs were combined to obtain their invariant mass. If these electron pairs come from J/ψ decay, their invariant mass is equal to the rest mass of J/ψ. There is a large combinatorial background originating from pairs which were combined by chance. Three methods have been used to reconstruct this background:

- **Like–sign method**: Electrons with same charge signs are combined within the same event.
- **Track rotation**: Invariant mass is reconstructed from electrons with unlike signs, where one of them has its momentum vector rotated by 180°.
- **Event mixing**: Electrons with opposite signs are combined, but coming from different events, Events used for combining should have similar properties, such as multiplicity and vertex z position.

The best description of combinatorial background was obtained by like–sign method. For this reason it is the method used for all following results.

Fig. 4.1 shows the invariant mass of unlike and like-sign pairs on the left panel. Right panel displays the signal after invariant mass of like-sign pairs has been subtracted from that of unlike-sign pairs. Even after the subtraction there is still some small background present in the data. This so called residual background is fitted with linear function. Crystal ball function

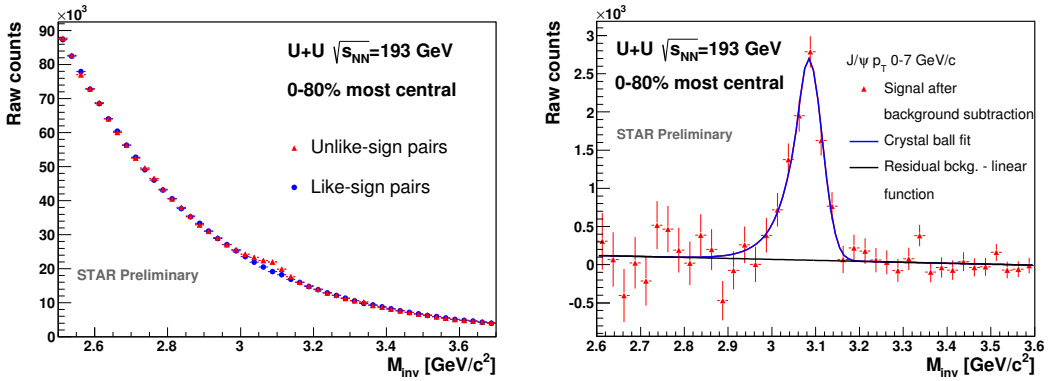

Figure 4.1: Left: Invariant mass of unlike-sign and like-sign electron (positron) pairs in 0-80 % most central U+U collisisons at $\sqrt{s_{NN}} = 193$ GeV. Right: Signal after background subtraction fitted with crystal ball function superimposed on a linear residual background.

is used to fit the actual signal:

$$f_{CB}(m) = \begin{cases} \frac{N}{\sqrt{2\pi}\sigma} \exp\left(-\frac{(m-m_0)^2}{2\sigma^2}\right) & \text{for } \frac{m-m_0}{\sigma} > -\alpha \\ \frac{N}{\sqrt{2\pi}\sigma} \left(\frac{n}{|\alpha|}\right)^2 \exp\left(-\frac{|\alpha|^2}{2}\right) \left(\frac{n}{|\alpha|} - |\alpha| - \frac{m-m_0}{\sigma}\right)^{-n} & \text{for } \frac{m-m_0}{\sigma} \leq -\alpha \end{cases} \tag{4.1}$$

It is a Gaussian with a tail, which accounts for electron radiation losses and also for J$\psi \to \gamma\, e^+e^-$ decay in which we are not able to detect the photon. The crystal ball function has 5 parameters: m_0 for mean, N is normalization constant, σ for width of the peak and n and α for describing the tail.

Statistical significance of signal is calculated as

$$Sg = \frac{S}{\sqrt{S + 2B}}, \tag{4.2}$$

where S is raw count of J/ψ in mass region (2.9-3.2) GeV/c^2 and B is background in the same mass region. We obtained significance 12.9 for 0-80 % most central collisions.

4.1 Signal p_{T} dependence

We have divided the J/ψ signal into 11 p_{T} bins going from 0 up to 7 GeV/c. Fig. 4.2 shows the changing shape of invariant mass in various p_{T} bins. Resulting signal after background subtraction with crystal ball + linear function fit is in Fig. 4.3.

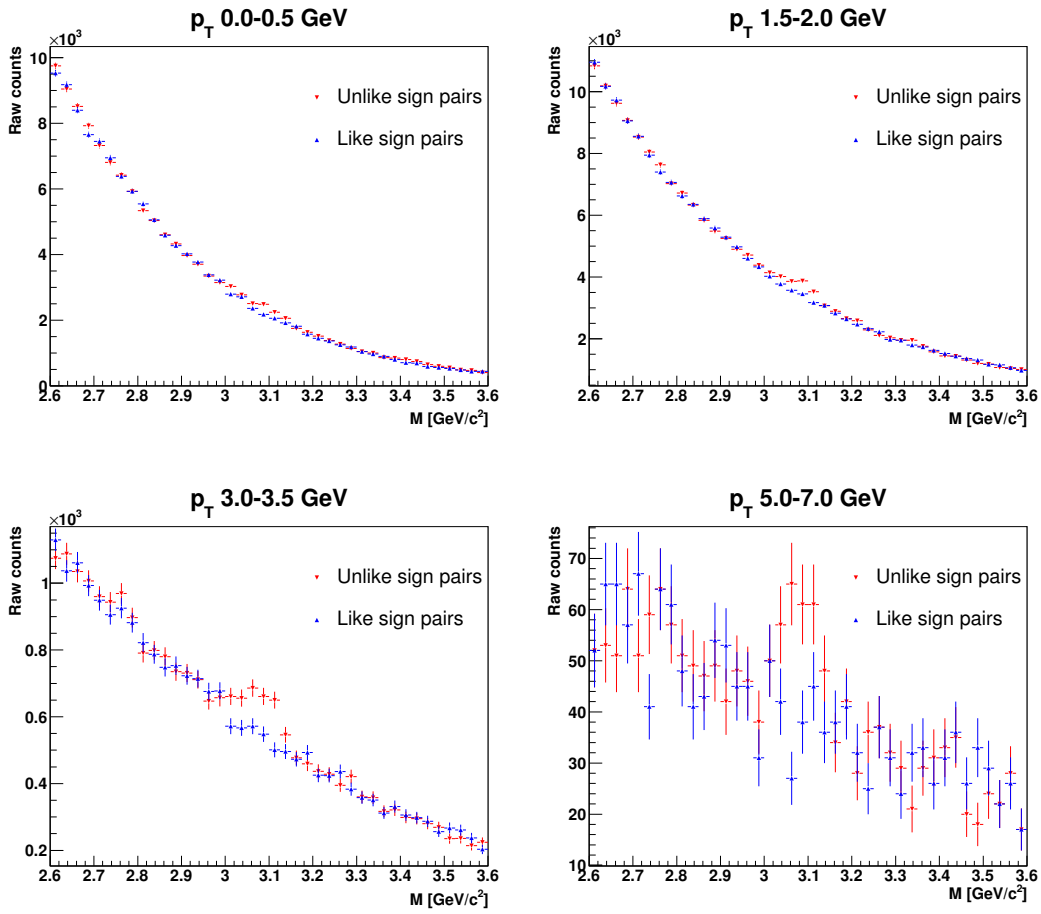

Figure 4.2: Invariant mass of unlike-sign and like-sign $e^-(e^+)$ pairs for several p_T bins.

Fig. 4.4 shows transverse momentum dependence of raw J/ψ yield. Significance of a signal in various p_T bins has been calculated according to Eq. 4.2 and can be seen in Fig. 4.5.

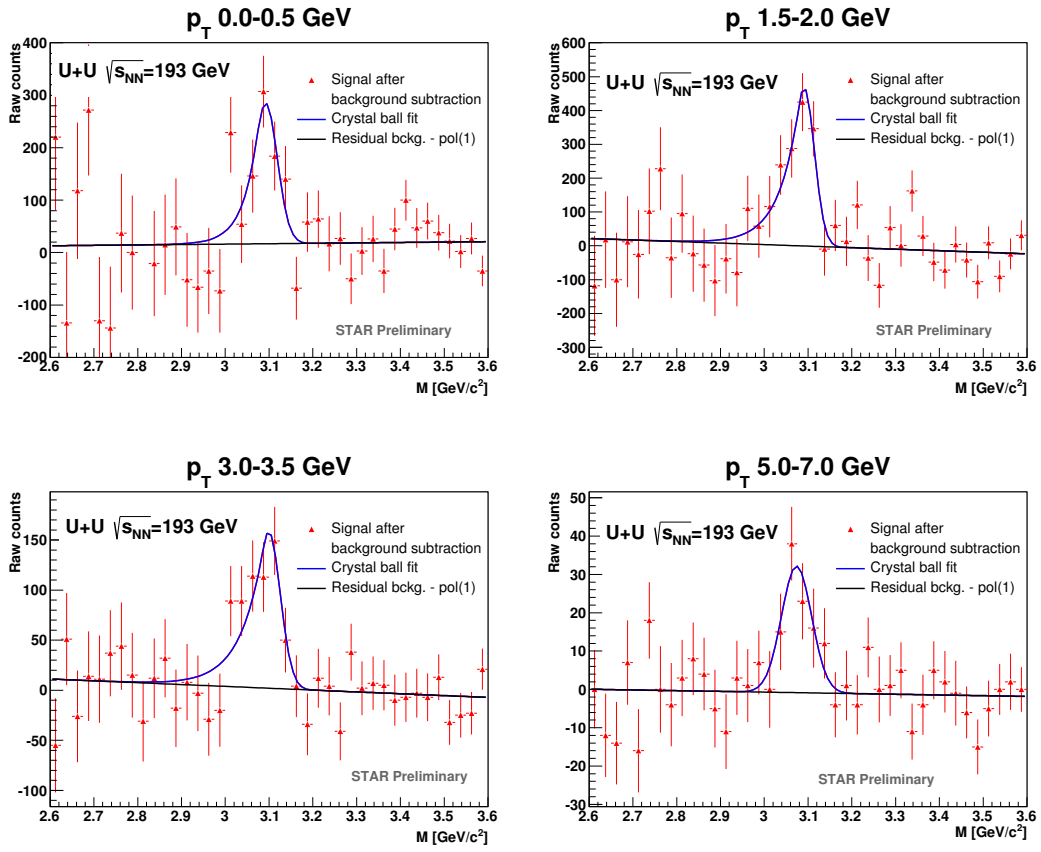

Figure 4.3: Signal after background subtraction for several p_T bins. Signal is then fitted with a crystal ball function, linear function is added to fit residual background.

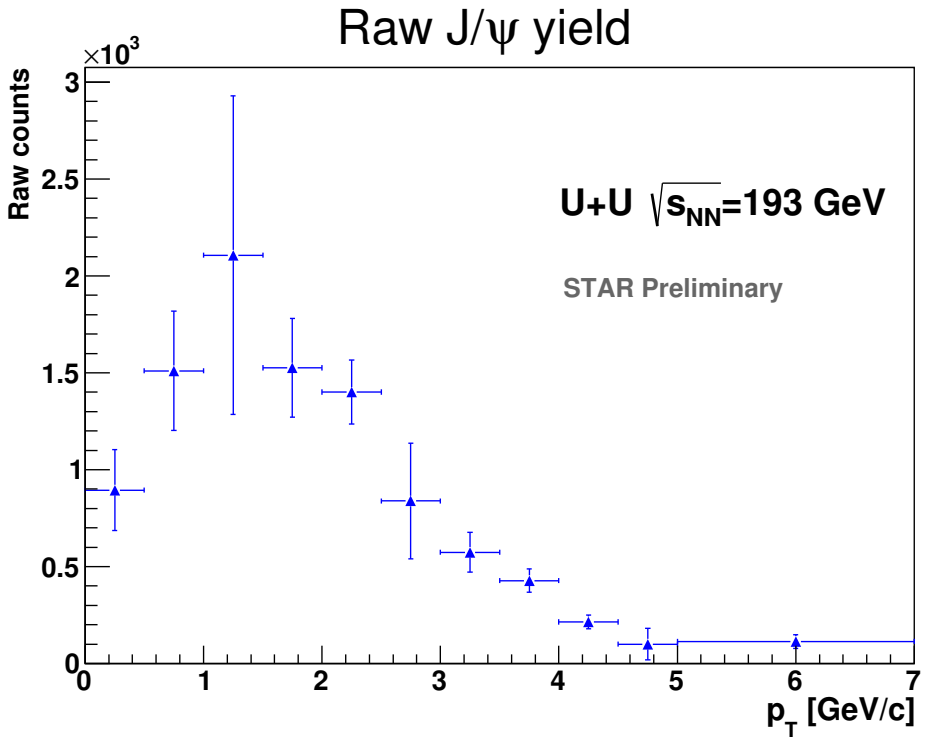

Figure 4.4: Dependence of raw J/ψ yield on transverse momentum for 0-80 % most central collisions.

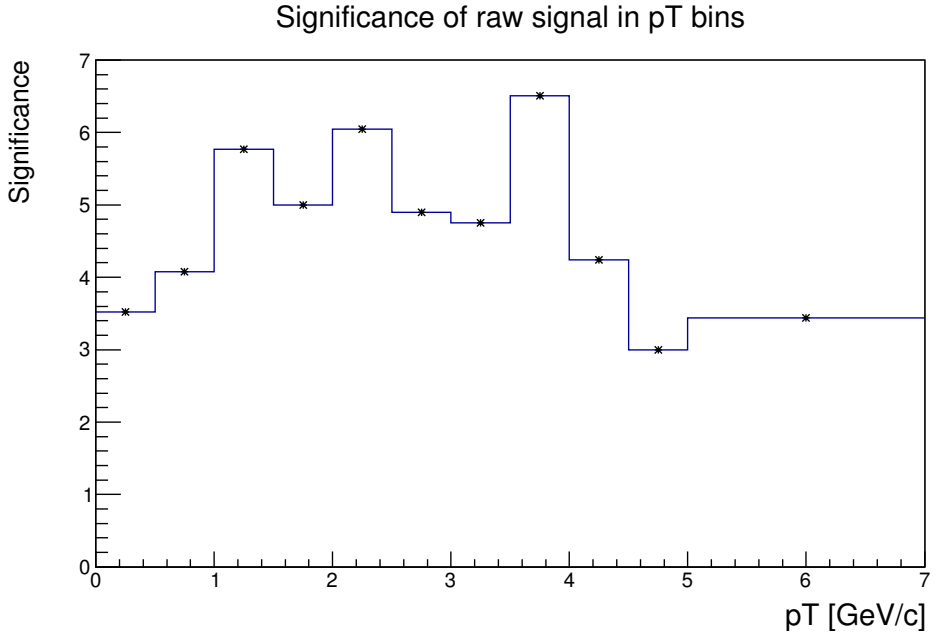

Figure 4.5: Significance of raw signal in p_{T} bins varies from 3.0 to 6.5.

4.2 Centrality dependence

J/ψ signal has been studied in the 0-10 % most central collisions (Fig. 4.6) and in the peripheral collisions (60-80 %, Fig. 4.7). Raw count in central collisions is higher than in peripheral, however combinatorial background is also much higher. This results in similar significance (calculated as 4.2) in both centralities. To further improve statistics for most central collisions, use of central triggers is planned.

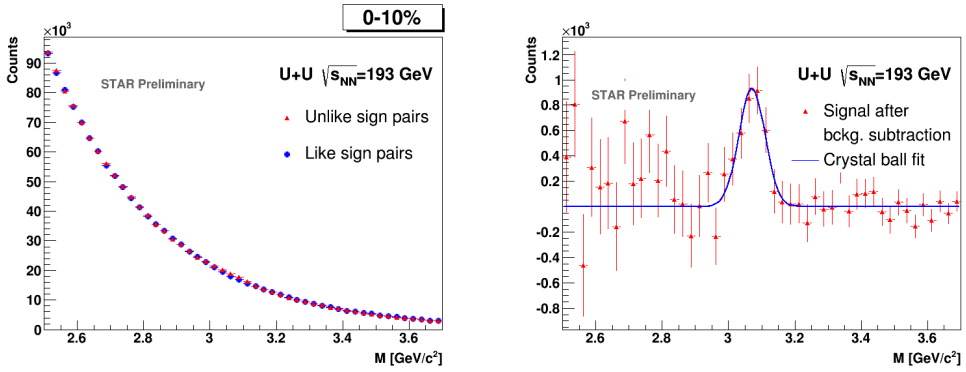

Figure 4.6: Left: Invariant mass of unlike and like-sign pairs for 0-10 % most central collisions. Right: Signal after background subtraction for 0-10 % most central collisions fitted with a crystal ball function.

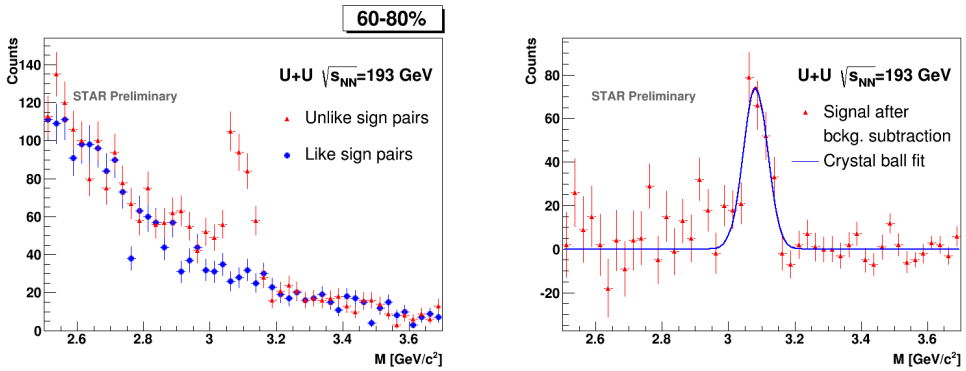

Figure 4.7: Left: Invariant mass of unlike and like-sign pairs for peripheral collisions (60-80 %). Right: Signal after background subtraction for centrality 60-80 %. Signal is fitted with a crystal ball function.

Chapter 5

Signal Corrections

The raw signal shown in chapter 4 needs to be corrected for all J/ψ that haven't been reconstructed by our analysis. There are two main groups of corrections. First is detector acceptance – the ratio between particles (e.g. electrons) registered in a given detector and all particles. The other is cut efficiency – the ratio of particles selected by our cut to all registered in the detector.

Corrections for this analysis are currently under way and only partially complete.

5.1 TPC

5.1.1 TPC cut efficiency

Electron $n\sigma_{\mathrm{e}}$ is required to be $-1.5 < n\sigma_e < 2.0$. The cut efficiency is obtained from data. First, pure electron sample without TPC cut is selected. This is tricky, as there is a significant hadron contamination. To reduce it only electron positron pairs with invariant mass lower then 12.5 MeV are used. These are expected to come from fotonic electrons (from γ conversion) and have higher chance that they are indeed electrons. In order to reduce hadron contamination even further, one electron from the candidate fotonic pair is required to fulfill TPC cut, and then the other one is saved. This way we can obtain sample pure enough even without using TPC for electron identification. The electron sample is then divided into momentum bins. In each bin, $n\sigma_e$ distribution of the specific ionization loss $\mathrm{d}E/\mathrm{d}x$ is fitted with two Gaussians, one describing electrons and the other remaining pion contamination. Fig. 5.1 shows the fit in two momentum bins. From the fit parameters, ratio of electrons which would pass the TPC cut to all electrons

is determined. Fig. 5.2 shows the resulting efficiency. The discontinuity around $p > 1.2$ GeV/c is non-physical remnant of event preselection and will have to be corrected in the future.

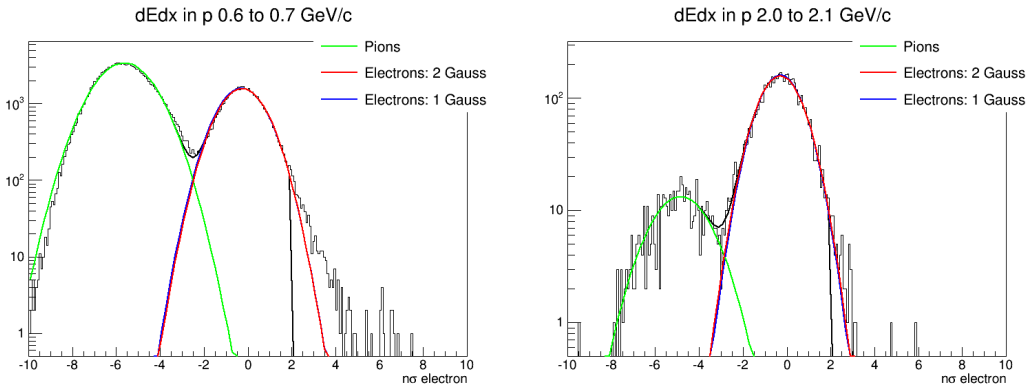

Figure 5.1: $n\sigma_e$ distribution for a pure electron sample for two momentum bins. Hadron contamination is still visible. The histogram is fitted with 2 Gaussians to describe electron and pion distribution.

5.1.2 TPC acceptance

TPC acceptance is obtained from embedding, where several J/ψ are generated in each collision and then their evolution in the detector is simulated. These simulated hits are then added to real events and the particles are reconstructed using the same cuts as in the analysis. Thus the number of simulated and also of reconstructed J/ψ is known. TPC acceptance can be obtained in this way. So far embedding for U+U collisions hasn't been done, but has already been requested for. It is expected to be finished within a couple of month.

5.2 TOF

5.2.1 TOF cut efficiency

Electrons are required to have $0,97 < 1/\beta < 1.03$. Cut efficiency for TOF is obtained by selecting a pure electron sample using only TPC and then determining how many of these electrons have fulfilled the TOF cut. Since the electron distribution is approximately Gaussian with width ≈ 0.007, cut is about 4σ away. Therefore the cut efficiency is very close to 1 as is shown in bottom right picture of Fig. 5.3.

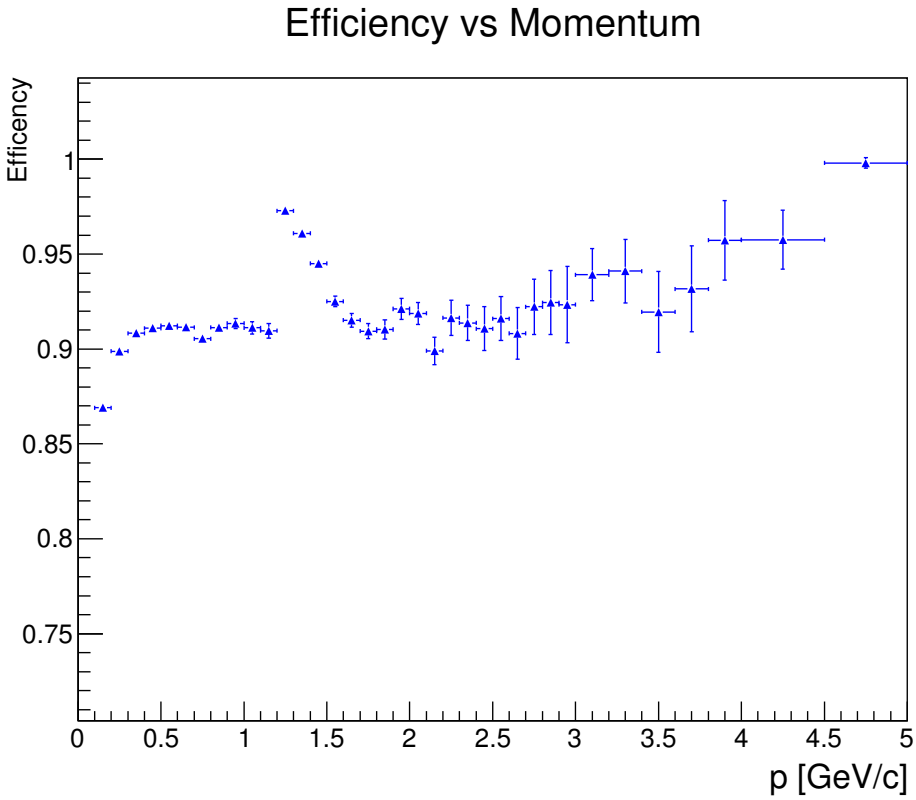

Figure 5.2: TPC cut efficiency as a function of electron momentum. The discontinuity for $p > 1.2$ GeV/c is caused by event preselection and will have to be corrected.

5.2.2 TOF acceptance

TOF acceptance is obtained from pure electron sample selected by TPC only. Then the ratio of electrons from this sample, which have a valid TOF signal, to all electrons is studied. Fig. 5.4 shows the centrality dependence, Fig. 5.5 describes pseudorapidity dependence. Only some of the errors are shown to make the pictures more organized.

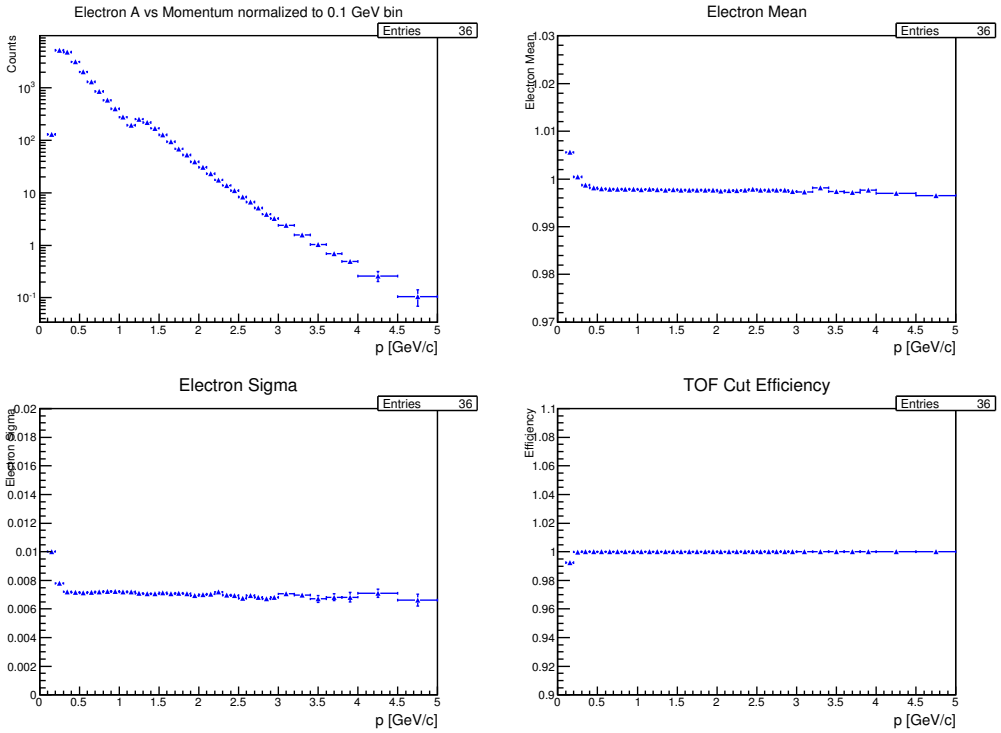

Figure 5.3: Top row and bottom left picture: parameters of Gaussian fit to distribution of 1β of pure electron sample. Right bottom: TOF cut efficiency as a function of momentum.

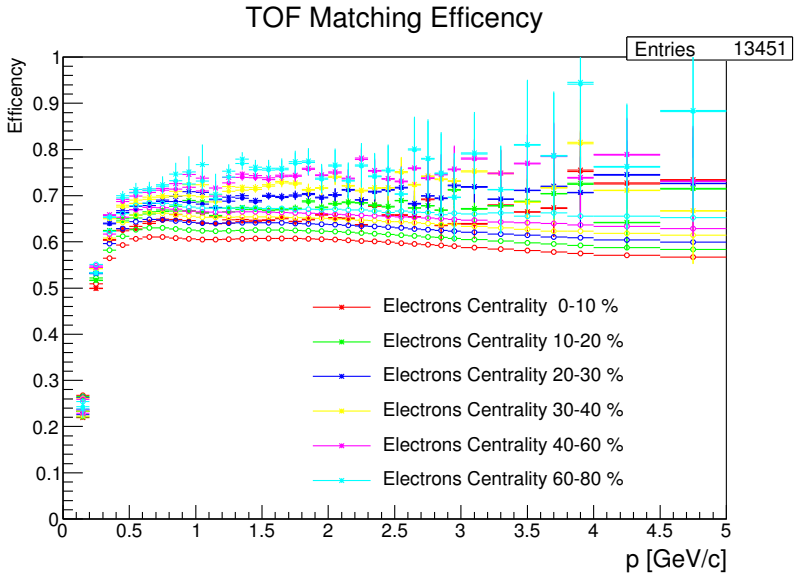

Figure 5.4: TOF acceptance for various centralities as a function of momentum.

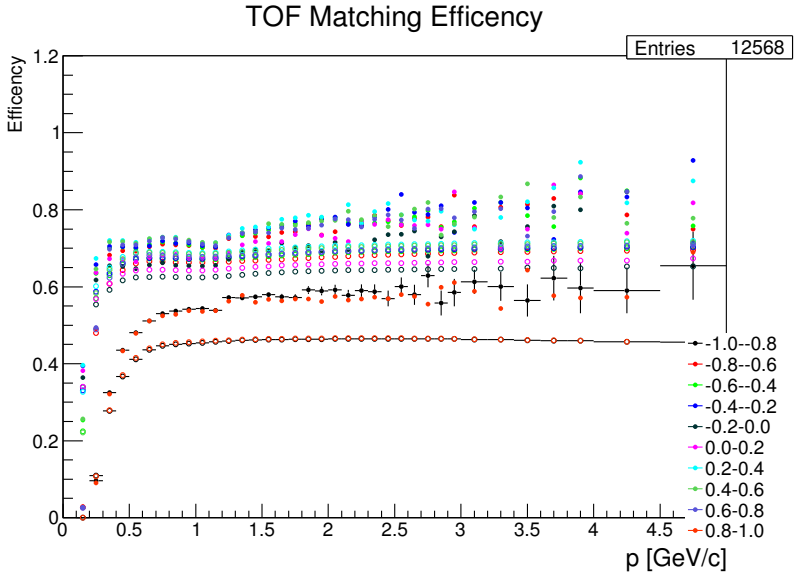

Figure 5.5: TOF acceptance for various pseudorapidities as a function of momentum. To improve clarity, errors are shown only for pseudorapidity -1.0 – -0.8. The errors are of similar magnitude for the remaining data points.

5.3 BEMC

So far, BEMC acceptance has been studied and is described below. BEMC cut efficiency can be obtained from data or from the simulations, the two approaches should give similar results.

5.3.1 BEMC acceptance

BEMC acceptance is obtained in the same manner as that of TOF. However, due to event preselection (described in 3.1.1), the electron sample for $p > 1.2$ GeV/c is biased toward those with BEMC signal. Hence the BEMC acceptance can not be used as it is, but has to be reworked without the bias caused by preselection, which remains to be done.

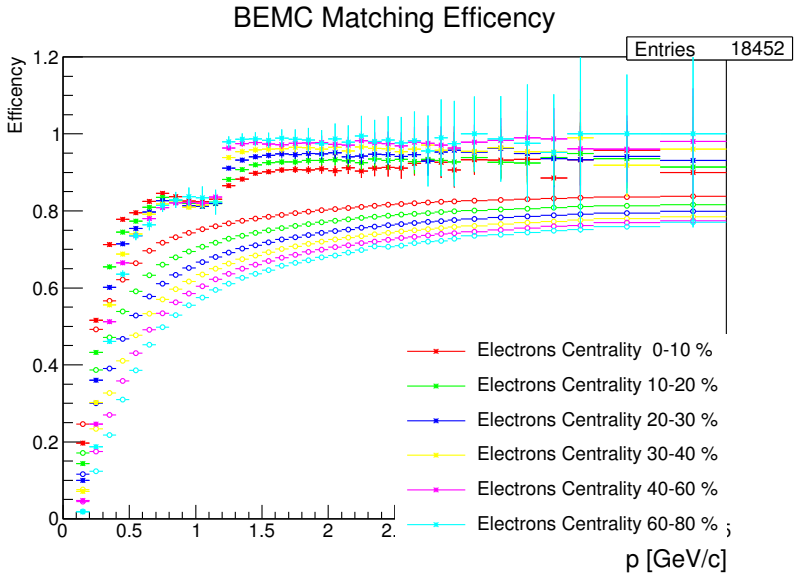

Figure 5.6: BEMC acceptance for various centralities as a function of momentum. The bump at 1.2 GeV/c is non-physical, caused by event preselection.

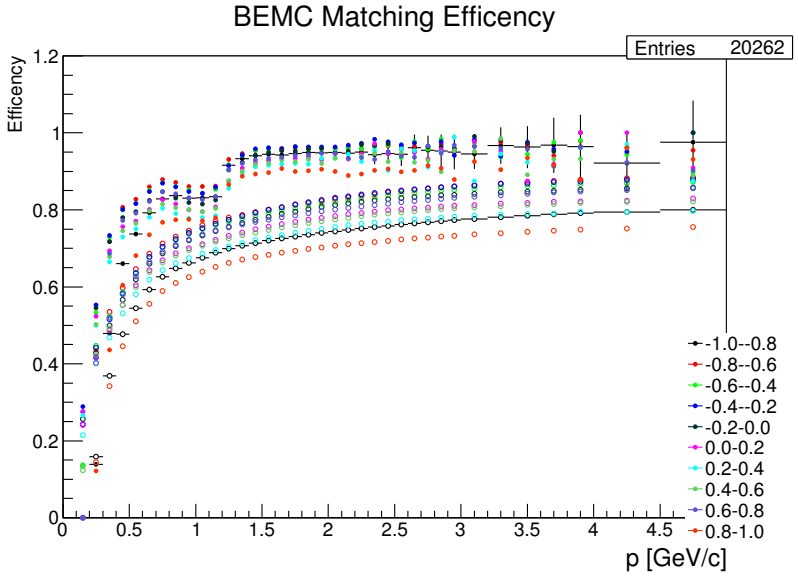

Figure 5.7: BEMC acceptance for various pseudorapidities as a function of momentum. The increase of acceptance at $p = 1.2$ GEV/c is caused by event preselection. Errors are shown only for pseudorapidity -1.0 – -0.8 in order to improve clarity. The errors are of similar magnitude for the remaining data points.

Conclusions and Outlook

In this analysis, $J/\psi \to e^+e^-$ in U+U collisions at $\sqrt{s_{NN}} = 193$ GeV at the STAR experiment has been studied. We have observed raw J/ψ signal with significance of 12.9 using information from TPC, TOF and BEMC detectors. This signal has been divided into several p_T bins and dependence of raw signal on p_T has been reported. Centrality dependence of the signal was also examined. First corrections of the raw yield were shown too.

Currently, work on efficiency studies and corrections of detector effects is being done. Then, cross section and nuclear modification factor R_{AA} as a function of centrality and p_T will be calculated. These measurement will thus improve our understanding of in-medium dissociation of heavy quarkonia and their role as the quark–gluon plasma thermometer.

The preliminary results of this analysis have already been presented at 2013 European Physical Society Conference on High Energy Physics, Stockholm, Sweden and published in Proceedings of Science. See Appendix for the work presented.

Bibliography

[1] T. Matsui and H. Satz, "J/psi Suppression by Quark-Gluon Plasma Formation," *Phys. Lett.*, vol. B178, 1986.

[2] R. Stock, "Relativistic Nucleus-Nucleus Collisions and the QCD Matter Phase Diagram," 2008. arXiv: 0807.1610.

[3] P. P. Bhaduri, P. Hegde, H. Satz, and P. Tribedy, "An Introduction to the Spectral Analysis of the QGP," *Lect.Notes Phys.*, vol. 785, pp. 179–197, 2010.

[4] X. Zhao and R. Rapp, "Charmonium in Medium: From Correlators to Experiment," *Phys.Rev.*, vol. C82, p. 064905, 2010.

[5] Y.-p. Liu, Z. Qu, N. Xu, and P.-f. Zhuang, "J/psi Transverse Momentum Distribution in High Energy Nuclear Collisions at RHIC," *Phys.Lett.*, vol. B678, pp. 72–76, 2009.

[6] Q. Hao and Star Collaboration, "Heavy Flavor Results from STAR," *Journal of Physics Conference Series*, vol. 422, p. 012013, Mar. 2013.

[7] L. Adamczyk *et al.*, "J/ψ production at high transverse momenta in $p+p$ and Au+Au collisions at $\sqrt{s_{NN}} = 200$ GeV," *Phys.Lett.*, vol. B722, pp. 55–62, 2013.

[8] B. Trzeciak, "Quarkonia production in the STAR experiment," *Nucl.Phys.A904-905*, vol. 2013, pp. 607c–610c, 2013.

[9] D. Kikola, G. Odyniec, and R. Vogt, "Prospects for quarkonia production studies in U + U collisions," *Phys.Rev.*, vol. C84, p. 054907, 2011.

[10] G. Wang, "Search for chiral magnetic effects in high-energy nuclear collisions," *Nuclear Physics A*, vol. 904-905, no. 0, pp. 248c – 255c, 2013.

[11] M. Anderson, J. Berkovitz, W. Betts, R. Bossingham, F. Bieser, *et al.*, "The Star time projection chamber: A Unique tool for studying high multiplicity events at RHIC," *Nucl.Instrum.Meth.*, vol. A499, pp. 659–678, 2003.

[12] STAR TOF Collaboration, "Proposal for a Large Area Time of Flight System for STAR," květen 2004.

[13] M. Beddo, E. Bielick, T. Fornek, *et al.*, "The STAR Barrel Electromagnetic Calorimeter," *Nucl.Instrum.Meth.*, vol. A499, pp. 725–739, 2003.

[14] C. Adler, A. Denisov, E. Garcia, M. J. Murray, H. Strobele, *et al.*, "The RHIC zero degree calorimeter," *Nucl.Instrum.Meth.*, vol. A470, pp. 488–499, 2001.

[15] W. Llope, F. Geurts, J. Mitchell, Z. Liu, N. Adams, *et al.*, "The TOFp / pVPD time-of-flight system for STAR," *Nucl.Instrum.Meth.*, vol. A522, pp. 252–273, 2004.

[16] M. L. Miller, K. Reygers, S. J. Sanders, and P. Steinberg, "Glauber modeling in high energy nuclear collisions," *Ann.Rev.Nucl.Part.Sci.*, vol. 57, pp. 205–243, 2007.

[17] H. Matsui, "Preliminary centrality definitions in U+U." Internal STAR presentation, May 2013.

Appendices

Part of the results of this analysis have been presented at 2013 European Physical Society Conference on High Energy Physics (EPS-HEP 2013) at Stockholm, Sweden, as a poster presentation and proceedings from the conference have been published at Proceedings of Science. These are included on following pages.

J/ψ production in U+U collisions at 193 GeV in the STAR experiment

Ota Kukral* for the STAR Collaboration

Faculty of Nuclear Sciences and Physical Engineering
Czech Technical University, Prague

Abstract

Extensive studies of properties of quark-gluon plasma (QGP), the partonic matter created in heavy ion collisions, have been conducted at RHIC for over a decade. Suppression of quarkonia production in high energy nuclear collisions relative to proton-proton collisions, due to Debye screening of the quark-antiquark potential, has been predicted to be a sensitive indicator of the temperature of the created QGP. However, initial-state nuclear effects on the parton distributions (shadowing), production via recombination of quark-antiquark pairs in the QGP and dissociation in hadronic phase could also alter the expected suppression picture. Systematic measurements of the quarkonia production for different colliding systems are required to understand the quarkonium interactions with the partonic medium, and then the QGP properties. To further study the pattern of quarkonia suppression we can utilize the collisions of non-spherical nuclei such as uranium.
In this poster, we present the analysis status on J/ψ production, reconstructed at midrapidity via di-electron decay channel, in U+U collisions at $\sqrt{s_{NN}}$ = 193 GeV in the STAR experiment.

Motivation

Measurements of J/ψ in-medium dissociation in heavy ion collisions are expected to provide an estimate of the initial temperature of the system. The interpretation of medium induced modification requires a good understanding of its production mechanisms in p+p collisions and cold nuclear matter effects in d+Au collisions.
In STAR, J/ψ was measured in p+p, d+Au, Au+Au [1] and Cu+Cu collisions at $\sqrt{s_{NN}}$ = 200 GeV and Au+Au collisions at $\sqrt{s_{NN}}$ = 39 GeV and 62 GeV.

- **Top picture** [2]: R_{AA} dependence on centrality of a collision for all p_T and for high p_T only. J/ψ suppression in Au+Au increases with a centrality and decreases toward higher p_T across the centrality range. The data are compared to models that include contributions from prompt production and statistical charm quark regeneration [3,4]
- **Bottom picture** [5]: Charged tracks multiplicity for Au+Au and U+U collisions. Top values of charged tracks multiplicity are higher in U+U collisions, which is caused by higher initial energy density (due to prolate shape of uranium nucleus).

Higher achievable energy density in uranium collisions could be used to further study quarkonia production [6].

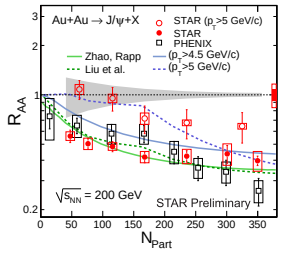

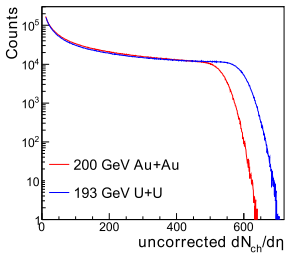

Data Analysis

Data used are 377M minimum bias uranium collisions at $\sqrt{s_{NN}}$ = 193 GeV taken in 2012.
Electrons are selected from good trajectories using TPC, TOF and BEMC:

TPC

- nσ - distance from the expected mean value of the energy loss expressed as number of standard deviations
- -1.5 < nσ electron < 2
- |nσ pion| > 2.5

TOF

- 0.97 < 1/β < 1.03
- Used: • p < 1.4 GeV/c — strictly required
  • p > 1.4 GeV/c — only if the particle has a TOF signal

BEMC

- Used only for p > 1.4 GeV/c
- 0.3 < p/E < 1.5

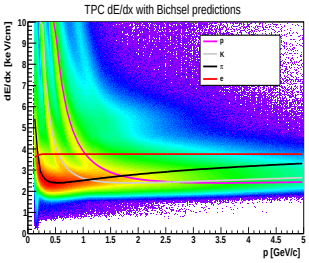

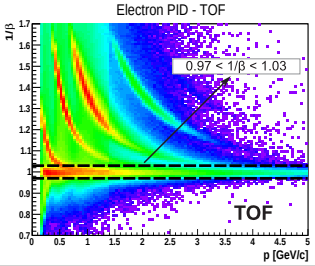

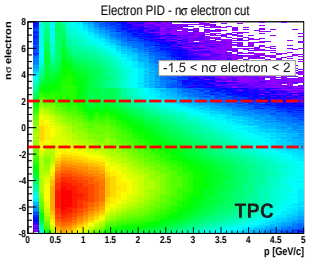

STAR Experiment

The Solenoidal Tracker At RHIC is a multi-purpose detector exceling at tracking and identification of charged particles at mid-rapidity in the high multiplicity environment of heavy ion collisions. The main subsystems used in this analysis are:

Time Projection Chamber (TPC)

- Full 2π azimuthal coverage
- Pseudorapidity -1.3 < η < 1.3
- Charged particle tracking and momentum reconstruction
- Particle identification via specific ionization energy loss dE/dx

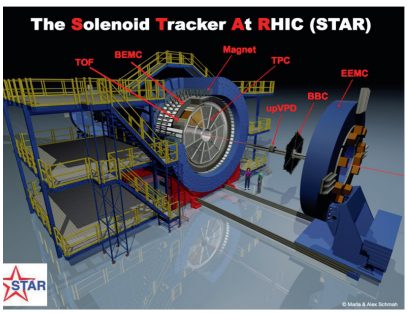

Time of Flight (TOF)

- Timing resolution <100 ps
- Particle identification via 1/β
- Together with TPC provides a good separation of electrons from heavier hadrons up to about 1.5 GeV/c

Barrel Electromagnetic Calorimeter (BEMC)

- Tower Δη×Δφ = 0.05×0.05
- Electron-hadron separation using p/E at high momentum

Results

- J/ψ → e^+e^- channel used for the analysis (branching ratio 5.9%)
- Combinatorial background reconstruction: Like-sign method ($e^+e^+ + e^-e^-$ pairs)
- Signal significance calculated in mass region (2.9 - 3.2) GeV/c^2 as $sg = \frac{S}{\sqrt{S+2B}}$
- S = 9440 ± 640 with significance 12.9 σ
- Signal divided into 11 p_T bins from 0 to 7 GeV/c with significance from 3.0 to 6.5 σ

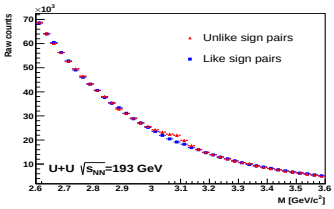

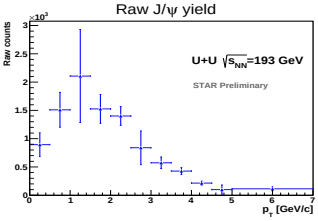

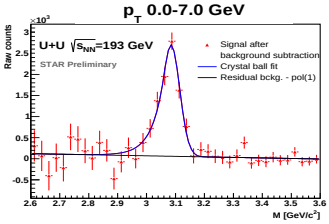

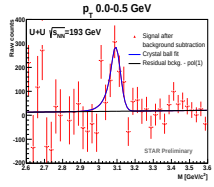

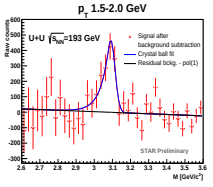

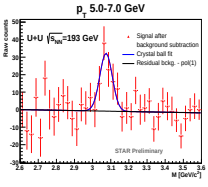

Conclusions and Perspectives

- J/ψ signal of significance of 12.9 σ observed
- Signal was divided into several p_T bins
- Studies of efficiency corrections and detectors effects are currently underway

References

[1] L. Adamczyk et al. [STAR Collaboration], Phys. Lett. B722, 55-62 (2013)
[2] H.Qiu (for the STAR Collaboration), J. Phys. Conf. Ser. 422, 012013 (2013)
[3] Y. Liu et al., Phys. Lett B678, 72 (2009)
[4] X. Zhao and R. Rapp, Phys. Rev. C82, 064905 (2010)
[5] G. Wang, Nuclear Physics A904–905, 248c-255c (2013)
[6] D. Kikola et al., Phys.Rev. C84,054907 (2011)

Acknowledgements

This work was supported by the grant of the Grant Agency of Czech Republic n. 13-20841S and by the Grant Agency of the Czech Technical University in Prague, grant No. SGS13/215OHK4/3T/14.

* kukral@rcf.rhic.bnl.gov.

Presented at the 2013 European Physical Society Conference on High Energy Physics, Stockholm, Sweden, 18-24 July, 2013

PROCEEDINGS OF SCIENCE

J/ψ production in U+U collisions at $\sqrt{s_{NN}} = 193$ GeV in the STAR experiment

Ota Kukral* **for the STAR Collaboration**
Department of Physics, Faculty of Nuclear Sciences and Physical Engineering, Czech Technical University in Prague, Czech Republic
E-mail: kukral@rcf.rhic.bnl.gov

Extensive studies of quark-gluon plasma (QGP), the novel state of strongly interacting matter governed by partonic degrees of freedom, have been conducted at RHIC for over a decade. Suppression of quarkonia production in high energy nuclear collisions relative to proton-proton collisions, due to Debye screening of the quark-antiquark potential, has been predicted to be a sensitive indicator of the temperature of the created QGP. However, cold nuclear matter effects, production via recombination of quark-antiquark pairs in the QGP and dissociation in hadronic phase could also alter the expected suppression picture. Indeed, recent measurements in Au+Au and d+Au collisions show that these effects play a non-negligible role. Hence systematic measurements of the quarkonia production for different colliding systems are crucial for understanding the quarkonium interactions with the partonic medium, and then the QGP properties. To further study the pattern of quarkonia suppression we can utilize the collisions of non-spherical nuclei such as uranium. In this paper, we will present the analysis status on J/ψ production, measured at midrapidity via di-electron decay channel, in U+U collisions at $\sqrt{s_{NN}} = 193$ GeV in the STAR experiment.

The European Physical Society Conference on High Energy Physics -EPS-HEP2013
18-24 July 2013
Stockholm, Sweden

*Speaker.

1. Motivation

Measurements of J/ψ in-medium dissociation in heavy ion collisions are expected to provide an estimate of the initial temperature of the system [1]. To understand medium induced modification it is beneficial to study J/ψ in various colliding systems. In STAR, J/ψ has been measured in p+p, d+Au, Au+Au and Cu+Cu collisions at $\sqrt{s_{NN}} = 200$ GeV [2][3] and Au+Au collisions at $\sqrt{s_{NN}} = 39$ GeV and 62 GeV [4]. U+U collisions are of interest since uranium nucleus is non-spherical, which leads to higher initial energy density not only in tip-to-tip collision, but even when averaged over all possible orientations of colliding nuclei [5][6].

2. Data Analysis

STAR is a multi-purpose detector excelling at tracking and identification of charged particles at mid-rapidity in the high multiplicity environment of heavy ion collisions. The main subsystems used for electron selection in this analysis are:

– Time Projection Chamber (TPC): momentum reconstruction together with particle identification via specific ionization energy loss $\mathrm{d}E/\mathrm{d}x$.
– Time of Flight (TOF): particle identification by measuring velocity β.
– Barrel Electromagnetic Calorimeter (BEMC): electron-hadron separation via momentum/energy ratio.

These results are based on analysis of 377 millions of minimum bias uranium collisions at $\sqrt{s_{NN}} = 193$ GeV taken in 2012 by the STAR experiment at RHIC. Sample of 0-80 % most central events with vertex z position within 30 cm of the center of the detector are used. Electrons were selected from good quality tracks by requiring $-1.5 < n\sigma_{\mathrm{electron}} < 2$ and $|n\sigma_{\mathrm{pion}}| > 2.5$ where $n\sigma$ is a distance from the expected mean value of the energy loss expressed as a number of standard deviations. The value of $1/\beta$ was required to be between 0.97 and 1.03. This cut has to be fulfilled for all particles with momentum lower then 1.4 GeV/c, for particles with p > 1.4 GeV/c the cut is applied only if they have a valid TOF signal. For particles with p > 1.4 GeV/c information from BEMC is also used for electron-hadron separation requiring the ratio 0.3 < p/E < 1.5, where E is an energy deposited by particle in a single BEMC tower. This takes advantage of the fact that electrons, unlike hadrons, deposit most of their energy in the calorimeter. Fig. 1 shows $n\sigma_{\mathrm{electron}}$ and $1/\beta$ distributions and applied cuts.

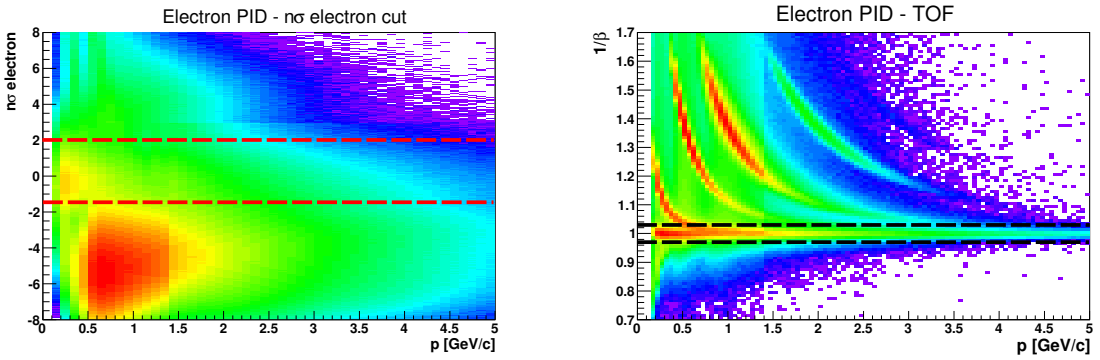

Figure 1: Left: TPC $n\sigma_{\mathrm{electron}}$ for particles which have already fulfiled TOF and BEMC cuts. Right: TOF $1/\beta$ vs. momentum for particles which have already passed TPC and BEMC cuts. Dashed lines show the selected region.

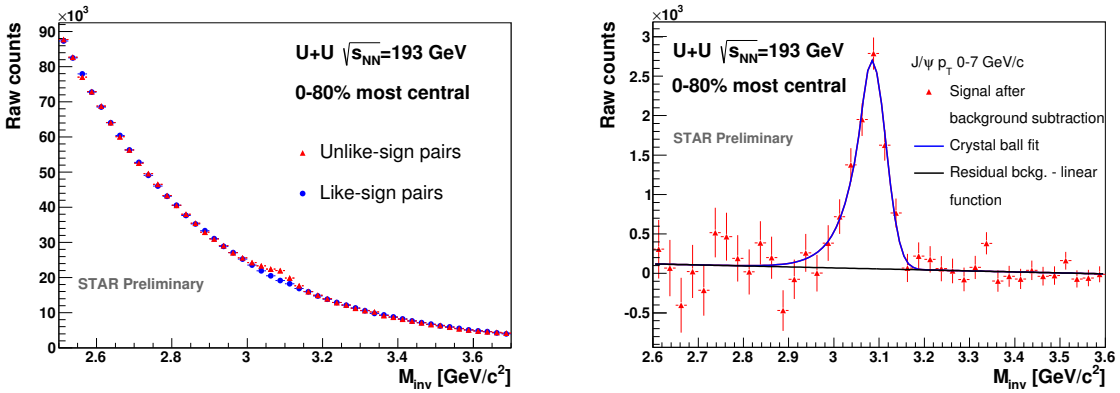

Figure 2: Left: Invariant mass of unlike-sign and like-sign electron (positron) pairs in 0-80 % most central U+U collisisons at $\sqrt{s_{NN}} = 193$ GeV. Right: Signal after background subtraction fitted with crystal ball function superimposed on a linear residual background.

3. Results and Summary

J/ψ is reconstructed via di-electron decay channel with branching ratio of 5.9 %. Combinatorial background is reconstructed using invariant mass of like-sign pairs. Signal after background subtraction is than fitted with crystal ball function to describe the signal and linear function to account for residual background. Signal before and after combinatorial background subtraction is shown on Fig. 2. Signal in mass region $(2.9-3.2)$ GeV/c^2 is 9440 ± 640 with significance of 12.9σ. This will make possible to divide the signal into several p_{T} bins going up to 7 GeV/c.

To conclude, in this work we have presented the current status of J/ψ analysis in U+U collisions at $\sqrt{s_{NN}} = 193$ GeV collected by the STAR experiment. Strong J/ψ signal has been observed in 0-80 % most central miminum bias collisions. This available statistics will allow us to extract nuclear modification factor $\mathrm{R_{AA}}$ as a function of p_{T} and centrality, therefore shedding more light on the effects associated with in-medium dissociation of heavy quarkonia.

Acknowledgments

This analysis was supported by the grant of the Grant Agency of Czech Republic n. 13-20841S and by the Grant Agency of the Czech Technical University in Prague, grant No. SGS13 /215OHK4/3T/14.

References

[1] T. Matsui and H. Satz, *J/psi Suppression by Quark-Gluon Plasma Formation*, Phys.Lett. **B178**, 416 (1986).

[2] L. Adamczyk et al. [STAR Collaboration], *J/ψ production at high transverse momenta in $p+p$ and Au+Au collisions at $\sqrt{s_{NN}} = 200$ GeV*, Phys.Lett. **B722**, 55-62 (2013).

[3] H. Qiu, *Heavy Flavor Results from STAR*, J.Phys.: Conf. Ser. **422** 012013 (2013).

[4] B. Trzeciak et al. [STAR Collaboration], *Quarkonia production in the STAR experiment*, Nucl.Phys. **A904-905**, 607c (2013).

[5] D. Kikola et al., *Prospects for quarkonia production studies in U+U collisions*, Phys. Rev. **C84** 054907 (2011).

[6] G. Wang, *Search for Chiral Magnetic Effects in High-Energy Nuclear Collisions*, Nucl.Phys. **A904-905**, 248c-255c (2013).